HHS Public Access

Author manuscript

J Glaucoma. Author manuscript; available in PMC 2021 October 01.

Published in final edited form as:

J Glaucoma. 2020 October ; 29(10): 857–863. doi:10.1097/IJG.0000000000001620.

Local glaucomatous defects of the circumpapillary retinal nerve fiber layer show a variety of patterns of progression.

Ha Min Kim, BA[1], **William E McKee, BA, BS**[1], **Kasia B. Malendowicz**[1], **Abinaya A. Thenappan, MD**[1,2], **Emmanouil Tsamis, PhD**[1], **Melvi D. Eguia, MD**[3], **C. Gustavo De Moraes, MD, MPH, PhD**[4], **Robert Ritch, MD**[3], **Donald C. Hood, PhD**[1,4]

[1]Department of Psychology, Columbia University, New York, NY, USA

[2]Columbia Vagelos College of Physicians and Surgeons, New York, NY, USA

[3]Einhorn Clinical Research Center, New York Eye and Ear Infirmary of Mount Sinai, New York, New York, USA

[4]Bernard and Shirlee Brown Glaucoma Research Laboratory, Department of Ophthalmology, Edward S. Harkness Eye Institute, Columbia University Irving Medical Center, New York, NY,, USA

Abstract

Purpose: To examine the patterns of circumpapillary retinal nerve fiber layer (cRNFL) loss secondary to glaucomatous progression in a region associated with the superior hemifield of the 24–2/30–2 visual field (VF).

Methods: 24 eyes (20 patients) with a diagnosis of glaucoma and evidence of progression on optical coherence tomography (OCT) had OCT disc cube scans on at least 3 separate visits (mean follow-up 7.4 years; range 3.9–11.4). Circumpapillary b-scans were derived after enface images were aligned to assure that the study region (i.e., 0° to −135°, where 0° is 9 o'clock, on a right eye) coincided. Within this region, a region of progression (ROP) was defined based on the loss in cRNFL thickness between the first and subsequent visits. The width of the ROP was determined, along with the locations of its leading (close to fixation) and trailing edges. In addition, for each ROP, the location and depth at the point of maximal loss, total loss, and average remaining RNFL were measured.

Results: The ROP proceeded both toward and away from fixation. Across eyes, the ROP varied widely in width (32° to 131°, mean 82.7°), location, and loss at point of deepest loss (22 to 99 μm, mean 52.9 μm), as well as total cRNFL loss.

Conclusion: All eyes showed a widening and deepening of the ROP, but a variety of different patterns of progressive cRNFL loss. Thus, one should expect considerable variation in patterns of

Correspondence: Donald C. Hood, Department of Psychology, 406 Schermerhorn Hall, 1190 Amsterdam Avenue, MC 5501, Columbia University, New York, NY 10027, USA. dch3@columbia.edu; Telephone: 212-854-4234; Fax: 212-854-3609.

Disclosure: H. M. Kim, None**; W. E. McKee**, None**; K. B. Malendowicz**, None**; A. A. Thenappan**, None**; E. Tsamis**, Topcon, Inc. (R); **M. D. Eguia**, None**; R. Ritch**: None; **D. C. Hood:** Heidelberg Engineering (R, F), Topcon, Inc. (R, F), Novartis (C, F).; **C. G. De Moraes**: Heidelberg Engineering (R), Topcon, Inc. (R), Novartis (C, F), Reichert (C), Carl Zeiss (R, C), Perfuse Therapeutics (C), Belite (C), Galimedix (C).

VF loss. Further, conventional metrics (global or quadrant cRNFL thickness) do not fully depict the progressive changes that can be appreciated by inspecting OCT images.

Précis:

The region of glaucomatous progression, seen on OCT images of the circumpapillary retinal nerve fiber layer, increases in width and depth in all eyes, but shows a variety of different patterns of loss across eyes.

Introduction

There is no litmus test for the detection of glaucoma or its progression. Thus, most clinicians use both functional (visual field) and structural/anatomical information. While traditionally the anatomical test was the fundus exam, typically with fundus photography, clinicians are increasingly using optical coherence tomography **(**OCT) along with visual fields for confirmation of progression.

The most common OCT analysis involves measurement of the thickness of the circumpapillary retinal nerve fiber layer (cRNFL) seen on circumpapillary b-scan images.[1] These b-scan images are either obtained from OCT circle scans or derived from OCT cube scans. In both cases, the cRNFL thickness is measured. Typically, the clinician looks at summary measures, such as the global average or the average of portions (e.g., quadrants) of the cRNFL thickness. These summary measures (called metrics here) can miss damage.[2–4] Moreover, these metrics ignore the information that can be obtained by looking at the actual circumpapillary b-scan image.[2]

We have argued that these images should be examined the way one would examine an MRI scan, namely by closely inspecting the details of the OCT b-scan image the way a radiologist would inspect an MRI image.[2,4] Examination of the cRNFL defects seen on b-scan images reveal a wide range of patterns of local damage, challenging the usefulness of trying to classify visual field patterns into particular groups.[5] In any case, Hood et al[5,6] argued that local defects can vary in location, depth, width and homogeneity of damage. However, relatively little is known about how these local defects change with progression.

The purpose of this study was to better understand how the cRNFL patterns of damage change as glaucoma progresses. In particular, we examined derived OCT circumpapillary b-scan images of eyes with clear evidence of progression over a period of at least 3 years. Furthermore, we focused on the region of the cRNFL associated with the superior portion of the 24–2/30–2 visual field, as this allowed us to align the scans obtained at different times in a region known to be prone to progression.[7–9]

Methods

Participants

Twenty-four eyes of 20 patients were selected from a large database with a diagnosis of glaucoma and spectral domain OCT (Topcon 3D-OCT 2000) cube scans of the disc obtained between August 2007 and July 2019. In particular, eyes were included if there was evidence

of progression in the region of study described below and if they met the following inclusion criteria: 3 or more years between the first and last OCT disc cube scans, and at least 3 separate visits with adequate scan quality. The time between the first and last visits ranged from 3.9 to 11.4 (mean 7.4± (SD) 2.6) years. At the first visit, the age of patients ranged from 32 to 74 (mean 57.6±11.5, median 61) years. Thirteen of the 20 patients were women and 7 were men. Mean deviation (MD) of a reliable 24–2 visual field closest in date with the first and last scans ranged from −8.19 to 1.7 (mean −2.06±2.12) dB, and −18.46 to 1.88 (mean −4.66±4.77) dB, respectively. The most recent clinical diagnoses were: 16 primary open angle glaucoma (POAG), 6 normal tension glaucoma (NTG), and 2 secondary glaucoma (1 pigmentary, 1 exfoliation glaucoma).

The Institutional Review Boards of Columbia University approved the study methodology, which adheres to the tenets of the Declaration of Helsinki and to the Health Insurance Portability and Accountability Act. Written informed consent was obtained from all participants involved in the study.

OCT analysis and Study Region

Region of study and progression reports: We chose to study a restricted region of the disc for two reasons. First, we were interested in variations in regions of the disc associated with the visual field tested with the 10–2 and 24–2 patterns. Second, due to head tilt and/or scanning artifacts it was not always possible to align the images of the scans from two tests (see below). Thus, we needed to study a smaller region. We chose to focus on the disc region associated with the superior 24–2/30–2 visual field, as it is the most common area damaged by glaucoma and includes a region associated with the macula.[5,10–14]

Figure 1 shows the derived circular b-scans (A,C) for two visits and the enface images with the location of the derived circle (B,D). Using a custom made MATLAB R2015a (MathWorks, Natick, MA) program, the enface images of disc cube scans from different sessions were aligned using blood vessel landmarks (blue arrows in Fig. 1B and D, corresponding to blue vertical lines in 1A and C) to assure that the study region (i.e., 0° to −135°, white arrow in panel A) of each scan coincided. This portion of the cRNFL includes the region associated with the superior hemifield of the 24–2 and 30–2 visual field.[5,15] Notice in Fig. 1 that the blood vessels are reasonably well aligned in the study region (blue vertical lines), while they are misaligned for the superior disc where the yellow vertical lines correctly fall on the shadows of the vessels in the lower panel (red arrows), but miss these in the upper panel (yellow arrows).

***Measuring changes in the region of progression (ROP)*:** The region of progression (ROP) was defined based upon the difference in cRNFL thickness between the first and subsequent visit. This is illustrated in Fig. 2 for a different eye than in Fig. 1. The upper panels (A,B) show the derived circle scans for the two visits and the enface images with the location of the derived circle scan superimposed (right panels of A and B). Figure 2C is a plot of the cRNFL thickness in the study region for the first (solid black curve) and Nth visit (dashed blue curve). The difference between them is shown as the light blue line at the bottom of Fig. 2C. This panel is enlarged as Fig 2D. The location and amount of loss at the

point of maximal loss (red arrow in Fig. 2C and 2D) was measured. Then starting from this point of maximal loss and moving along the difference curve to the left (blue dashed arrow, Fig. 2D) and to the right (orange dashed arrow, Fig. 2D), the leading (close to fixation, blue arrow) and trailing edges (orange arrow) were defined as the first location on the difference curve which fell below −5 μm. The width of the ROP was taken as the distance (in degrees) between the leading and trailing edges.

Total loss in the ROP was also measured (hatched region, Fig. 2D) by calculating the area, in μm^2, under the difference curve starting and ending at the first points on the curve which fell below −5 μm. The average RNFL thickness at the last scan date was also calculated for each eye.

Results

Variations in region of progression (ROP) between first and last scans

The hatched region in Fig. 2D shows the cRNFL loss in the ROP between the first and last scans. This region of loss is shown in Fig. 3 for each of the 24 eyes. Each curve represents the difference curve of an eye (i.e. light blue curve in Fig. 2D), ordered according to location of the point of maximal loss. Black indicates clinical diagnosis of POAG; red indicates NTG, and blue secondary glaucoma (pigmentary or exfoliation glaucoma).

ROP Width: The width of the ROP, which is the width of the curves in Fig. 3, ranged from 32° to 131° (mean 82.7°±27.1°). This represented between 24% and 97% of the entire study region. Even after correction for time between the first and last scans, the change in width of the ROP varied over a large range, from 2.6% to 16.9% of the study region per year.

ROP depth: In all eyes, the ROP widened with concurrent deepening. No eyes showed widening without deepening. However, there was a large variation in the location and depth of the point of maximal loss. The red circles in Fig. 3 show the location of maximal loss, which varied from −38° to −112°. The amount of loss at the location of maximal loss ranged from 22 to 99 μm (mean 52.9±20.4 μm). After adjusting for time, the wide range of depths persisted.

ROP Total cRNFL loss: There was also a wide range of total cRNFL loss. Total cRNFL loss in the ROP between the first and last scans (hatched area under curve in Fig. 1) ranged from 27,090 to 134,185 μm^2 (mean 67,997.9±32,182.4 μm^2). After adjustment for time, the wide variation in total loss per year, which was more than a factor of 6, persisted.

Direction of progression relative to fixation: All 24 eyes had at least 3 scan dates from which we could determine whether progression proceeded toward or away from the location on the disc associated with fixation (approximately 0°, or 9 o'clock on right eye). Figure 4 shows an example of an eye with progressive loss of cRNFL both towards 0° (leading edge) and in the opposite direction (trailing edge). The initial edges of the ROP are shown as the gray dashed (leading edge) and solid (trailing edge) vertical lines, and the final edges as the dark blue vertical dashed and solid lines. The dark blue solid line shows extension of the trailing edge past the study region (−135°). The ROPs of 16 of the 24 eyes

(67%) increased in width both towards and away from fixation, while 5 increased just towards fixation (21%), and 3 (12%) only away from fixation.

Variations in ROP patterns of cRNFL loss

The results above suggest a wide range of variation in patterns of progression in width, loss at location of maximal loss, and total loss in the ROP. To illustrate and confirm this variation, we compared patterns of loss for eyes with similar ROP width, ROP total loss, and RNFL remaining in the study region at the last scan date.

Similar ROP width but different patterns: The 3 eyes represented in Fig. 5A–C all had an ROP with similar width (99.5° to 106.2°), but different patterns of loss. Notice, for example, the variation in the width, number, and location of particularly deep regions of loss (white arrows).

Similar ROP total loss but different patterns: Eyes with similar ROP total loss also showed a variety of patterns of loss as seen in Fig. 5D–F. Figure 5D shows wide loss which becomes deeper away from fixation. Figure 5E shows approximately equal depth across the ROP. Figure 5F shows a single deep area of local loss which is less wide than D or E.

Similar average thickness remaining in study region but different patterns of RNFL: Eyes with similar average cRNFL thicknesses at the last scan dates also demonstrated widely varying patterns of loss as illustrated in Fig. 5G–I. The depth of local loss, as well as the width of the ROP varies in these eyes. Fig. 5G demonstrates greatest loss (white arrow) towards 0° relative to the blood vessel, while Fig. 5H shows loss on either side of blood vessels, and Fig. 5I shows loss on the side of the blood vessels away from 0°.

Discussion

The purpose of this study was to better understand the patterns of change in OCT cRNFL as glaucoma progresses. We have previously argued that at any point in time there was a wide range of patterns of glaucomatous damage,[5] even in eyes with similar 24–2 mean deviations. Here we report that the change over time, progression, also shows a wide range of patterns. In particular, the region of progression (ROP) within the 135° region studied shows marked variation in width, depth, amount and location of maximum cRNFL loss, average cRNFL remaining, as well as heterogeneity of damage. These findings underscore the limitations of conventional metrics (global or quadrant cRNFL thickness) in fully depicting progressive changes seen with OCT.

While methods for evaluating the glaucomatous progression of cRNFL through average thickness measurements have been well-studied,[1,16–19] patterns of cRNFL progression have not been studied. Studies using global and sectoral average cRNFL thickness measurements to track progression of glaucoma have highlighted that glaucomatous damage in the inferotemporal sector, which is included in our region of study, is most vulnerable to progression.[7–9,20] Other studies, which explore patterns of progression through fundus photography and/or OCT, have found an increased tendency of progressive widening of

glaucomatous defects towards fixation more than away, and widening with concomitant deepening of loss.[6,17]

Our results are consistent with the general framework that progression primarily occurs through widening and deepening of existing defects.[22] Even taking into consideration the uncertainty of defining exactly the start and end of the ROP, it is clear there is a wide variation in width. In addition, we provide evidence for four other general features of progression. One, progression occurs over a relatively wide region. It is rarely a very local phenomenon. Two, it occurs both toward and away from the region associated with fixation. Three, there is wide variation in the pattern of loss even in our study region, which covers less than 40% of the disc. As the ROP can vary in location, width, depth, and heterogeneity of loss over time, simple metrics such loss of global or quadrant or clock hour cRNFL thickness will not capture the nature of the loss in cRNFL. Thus, these observations point to the need for the clinician to closely examination OCT images (b-scans), as well as the thickness and probability maps, in order to understand the nature and location of progression for any given eye.

Implications for visual field changes

Relatively little is known about the patterns of visual field loss as glaucoma progresses. Suh et. al[21] found patterns of visual field progression which were compatible with patterns of cRNFL loss seen on fundus photography, namely deepening, widening of an existing scotoma, and appearance of a new scotoma. Boden et. al report that most common visual field progression patterns are expansion alone, deepening alone, and combination of expansion and deepening.[22] Other studies have reported various rates and patterns of symmetric and asymmetric visual field changes in glaucoma patients and identified the superonasal quadrant as most vulnerable to glaucomatous damage,[14,23–25] a region of the field associated with our region of study. There have also been recent attempts to categorize discrete patterns of visual field progression into identifiable archetypes.[12] Our results, in conjunction with studies showing good correlation between cRNFL and visual field progression,[26,27] argue against discrete visual field archetypes, as well as a simple deepening of a defect without a widening.

What should the changes in the pattern of damage seen on visual fields look like based upon the variation in ROP describe here? First, recall that our region of study includes the portion of the cRNFL associated with the entire superior region of the 10–2 and 24–2/30–2 visual field patterns.[3] Second, there is excellent topographical agreement between cRNFL loss and visual field loss,[9] as long as both 10–2 and 24–2/30–2 tests are performed.[28,29] Thus, we predict that the pattern of cRNFL loss should, on average, be reflected in the pattern of visual field loss in the associated region. In particular, wider and deeper visual field defects are to be expected. However, in addition we should expect wide variations in the spatial patterns of local visual field loss within the affected regions, and these variations should, on average, be predictable from the changes in the OCT ROP. Consistent with this prediction are our earlier studies[30,31] which showed that eyes with regions of nearly complete cRNFL loss had visual field losses worse than −15 dB in the corresponding field locations.

Directions for further study include comparing patterns of cRNFL progression with changes in the thickness of the OCT ganglion cell layer, as well as changes in visual field sensitivity.[32,33] While a thorough investigation of the correlation between cRNFL and visual field progression are out of the scope of this project, examples from available data in this project corroborate what has been reported, that cRNFL progression is associated with expansion and deepening of visual field defects.

Limitations

The most obvious limitation is the sample size of 24 eyes, which was restricted by the inclusion criteria. To be selected, an eye had to progress, and have scans that could be aligned from at least 3 test days over a period of more than 3 years. However, a larger sample is not likely to lead to less variation. On the other hand, a larger sample would allow us to ask if the type of glaucoma (e.g., POAG vs. secondary) affect the pattern of damage.

A second limitation is the impact of blood vessels on the pattern of loss in the ROP. Clearly, blood vessels influence this pattern and more sophisticated methods will need to be devised to understand this influence. We can, however, rule out the simple model that would invalidate our conclusions. This model assumes that the loss is the same everywhere, say 25% of cRNFL in the region of study. Because glaucoma has a relatively small effect on blood vessel size[35] this model predicts variation in patterns of ROP even with a homogeneous loss of cRNFL. However, the examples supplied in Fig. 5 clearly rule out this simple model. Furthermore, a wide variety of patterns of local damage can be seen on either or both sides of vessels, or in regions without prominent blood vessels (Fig. 5).

Conclusions

The region of the cRNFL studied included the 135° portion of the disc that is associated with the superior 24–2 /30–2 visual field locations. The loss of cRNFL within this region proceeds both toward and away from the location of the cRNFL associated with the macula and fixation. While all eyes showed a widening and deepening of the region of progression, this region also showed a wide variety of patterns of cRNFL loss over time across eyes. Thus, one should expect considerable variation in patterns of VF loss from eye to eye. In addition, conventional metrics (global or quadrant cRNFL thickness) do not fully depict the progressive changes that can be appreciated by inspecting OCT images.

Acknowledgments

Funding: Supported in part by the Joseph and Marilyn Rosen Research Fund of the New York Glaucoma Research Institute, New York, NY, and by National Institutes of Health grants EY-02115 (DCH) and EY-025253 (CGDM).

References

1. Tatham AJ, Medeiros FA. Detecting Structural Progression in Glaucoma with Optical Coherence Tomography. Ophthalmology. 2017;124(12):S57–S65. doi:10.1016/j.ophtha.2017.07.015 [PubMed: 29157363]
2. Hood DC, De Moraes CG. Four Questions for Every Clinician Diagnosing and Monitoring Glaucoma. J Glaucoma. 2018;27(8):657–664. doi:10.1097/IJG.0000000000001010 [PubMed: 29917000]

3. Wang DL, Raza AS, de Moraes CG, et al. Central Glaucomatous Damage of the Macula Can Be Overlooked by Conventional OCT Retinal Nerve Fiber Layer Thickness Analyses. Transl Vis Sci Technol. 2015;4(6):4. doi:10.1167/tvst.4.6.4
4. Hood DC, de Moraes CG. Challenges to the common clinical paradigm for diagnosis of glaucomatous damage with OCT and visual fields. Investig Ophthalmol Vis Sci. 2018;59(2):788–791. doi:10.1167/iovs.17-23713 [PubMed: 29392325]
5. Hood DC. Improving our understanding, and detection, of glaucomatous damage: An approach based upon optical coherence tomography (OCT). Prog Retin Eye Res. 2017;57:46–75. doi:10.1016/j.preteyeres.2016.12.002 [PubMed: 28012881]
6. Hood DC, Wang DL, Raza AS, de Moraes CG, Liebmann JM, Ritch R. The Locations of Circumpapillary Glaucomatous Defects Seen on Frequency-Domain OCT Scans. Investig Opthalmology Vis Sci. 2013;54(12):7338. doi:10.1167/iovs.13-12680
7. Leung CKS, Yu M, Weinreb RN, Lai G, Xu G, Lam DSC. Retinal nerve fiber layer imaging with spectral-domain optical coherence tomography: Patterns of retinal nerve fiber layer progression. Ophthalmology. 2012;119(9):1858–1866. doi:10.1016/j.ophtha.2012.03.044 [PubMed: 22677426]
8. Xu G, Weinreb RN, Leung CKS. Retinal nerve fiber layer progression in glaucoma: A comparison between retinal nerve fiber layer thickness and retardance. Ophthalmology. 2013;120(12):2493–2500. doi:10.1016/j.ophtha.2013.07.027 [PubMed: 24053994]
9. Kim HJ, Jeoung JW, Yoo BW, Kim HC, Park KH. Patterns of glaucoma progression in retinal nerve fiber and macular ganglion cell-inner plexiform layer in spectral-domain optical coherence tomography. Jpn J Ophthalmol. 2017;61(4):324–333. doi:10.1007/s10384-017-0511-3 [PubMed: 28374270]
10. Hood DC, Raza AS, Gustavo C, Moraes V De, Liebmann JM, Ritch R. Progress in Retinal and Eye Research Glaucomatous damage of the macula. Prog Retin Eye Res. 2013;32:1–21. doi:10.1016/j.preteyeres.2012.08.003 [PubMed: 22995953]
11. Hood DC, Raza AS. Method for comparing visual field defects to local RNFL and RGC damage seen on frequency domain OCT in patients with glaucoma. Biomed Opt Express. 2011;2(5):1097. doi:10.1364/boe.2.001097 [PubMed: 21559122]
12. Hood DC, Raza AS, de Moraes CG V., et al. Initial arcuate defects within the central 10 degrees in glaucoma. Investig Ophthalmol Vis Sci. 2011;52(2):940–946. doi:10.1167/iovs.10-5803 [PubMed: 20881293]
13. Artes PH, Chauhan BC. Longitudinal changes in the visual field and optic disc in glaucoma. Prog Retin Eye Res. 2005;24:333–354. doi:10.1016/j.preteyeres.2004.10.002 [PubMed: 15708832]
14. Pereira MLM, sik Kim C, Zimmerman MB, Alward WLM, Hayreh SS, Kwon YH. Rate and pattern of visual field decline in primary open-angle glaucoma. Ophthalmology. 2002;109(12):2232–2240. doi:10.1016/S0161-6420(02)01248-4 [PubMed: 12466164]
15. Garway-Heath DF, Poinoosawmy D, Fitzke FW, Hitchings RA. Mapping the visual field to the optic disc in normal tension glaucoma eyes. Ophthalmology. 2000;107(10):1809–1815. doi:10.1016/S0161-6420(00)00284-0 [PubMed: 11013178]
16. Na JH, Sung KR, Baek S, et al. Detection of glaucoma progression by assessment of segmented macular thickness data obtained using spectral domain optical coherence tomography. Investig Ophthalmol Vis Sci. 2012;53(7):3817–3826. doi:10.1167/iovs.11-9369 [PubMed: 22562510]
17. Medeiros FA, Zangwill LM, Alencar LM, et al. Detection of glaucoma progression with stratus OCT retinal nerve fiber layer, optic nerve head, and macular thickness measurements. Investig Ophthalmol Vis Sci. 2009;50(12):5741–5748. doi:10.1167/iovs.09-3715 [PubMed: 19815731]
18. Na JH, Sung KR, Lee JR, et al. Detection of glaucomatous progression by spectral-domain optical coherence tomography. Ophthalmology. 2013;120(7):1388–1395. doi:10.1016/j.ophtha.2012.12.014 [PubMed: 23474248]
19. Diniz-Filho A, Abe RY, Zangwill LM, et al. Association between Intraocular Pressure and Rates of Retinal Nerve Fiber Layer Loss Measured by Optical Coherence Tomography In: Ophthalmology. Vol 123 Elsevier Inc.; 2016:2058–2065. doi:10.1016/j.ophtha.2016.07.006 [PubMed: 27554036]
20. Sung KR, Kim S, Lee Y, Yun SC, Na JH. Retinal nerve fiber layer normative classification by optical coherence tomography for prediction of future visual field loss. Investig Ophthalmol Vis Sci. 2011;52(5):2634–2639. doi:10.1167/iovs.10-6246 [PubMed: 21282570]

21. Suh MH, Kim DM, Kim YK, Kim TW, Park KH. Patterns of progression of localized retinal nerve fibre layer defect on red-free fundus photographs in normal-tension glaucoma. Eye. 2010;24(5):857–863. doi:10.1038/eye.2009.209 [PubMed: 19680281]
22. Boden C, Blumenthal EZ, Pascual J, et al. Patterns of glaucomatous visual field progression identified by three progression criteria. Am J Ophthalmol. 2004;138(6):1029–1036. doi:10.1016/j.ajo.2004.07.003 [PubMed: 15629296]
23. Miki A, Medeiros FA, Weinreb RN, et al. Rates of retinal nerve fiber layer thinning in glaucoma suspect eyes. Ophthalmology. 2014;121(7):1350–1358. doi:10.1016/j.ophtha.2014.01.017 [PubMed: 24629619]
24. O'Brien C, Schwartz B, Takamoto T, Wu DC. Intraocular Pressure and the Rate of Visual Field Loss in Chronic Open-Angle Glaucoma. Am J Ophthalmol. 1991;111(4):491–500. doi:10.1016/S0002-9394(14)72386-4 [PubMed: 2012152]
25. Susanna BN, Ogata NG, Daga FB, Susanna CN, Diniz-Filho A, Medeiros FA. Association between Rates of Visual Field Progression and Intraocular Pressure Measurements Obtained by Different Tonometers. Ophthalmology. 2019;126(1):49–54. doi:10.1016/j.ophtha.2018.07.031 [PubMed: 30114419]
26. Sehi M, Zhang X, Greenfield DS, et al. Retinal nerve fiber layer atrophy is associated with visual field loss over time in glaucoma suspect and glaucomatous eyes. Am J Ophthalmol. 2013;155(1):73–82.e1. doi:10.1016/j.ajo.2012.07.005 [PubMed: 23036570]
27. Yu M, Lin C, Weinreb RN, Lai G, Chiu V, Leung CKS. Risk of Visual Field Progression in Glaucoma Patients with Progressive Retinal Nerve Fiber Layer Thinning A 5-Year Prospective Study. Ophthalmology. 2016;123(6):1201–1210. doi:10.1016/j.ophtha.2016.02.017 [PubMed: 27001534]
28. Hood DC, Tsamis E, Bommakanti NK, et al. Structure-function agreement is better than commonly thought in eyes with early glaucoma. Investig Ophthalmol Vis Sci. 2019;60(13):4241–4248. doi:10.1167/iovs.19-27920 [PubMed: 31618760]
29. Tsamis E, Bommakanti NK, Sun A, Thakoor KA, De Moraes CG, Hood DC. An Automated Method for Assessing Topographical Structure–Function Agreement in Abnormal Glaucomatous Regions. Transl Vis Sci Technol. 2020;9(4):14. doi:10.1167/tvst.9.4.14
30. Mavrommatis MA, Wu Z, Naegele SI, et al. Deep defects seen on visual fields spatially correspond well to loss of retinal nerve fiber layer seen on circumpapillary OCT scans. Investig Ophthalmol Vis Sci. 2018;59(2):621–628. doi:10.1167/iovs.17-23097 [PubMed: 29392306]
31. Hood DC, Kardon RH. A framework for comparing structural and functional measures of glaucomatous damage. Prog Retin Eye Res. 2007;26(6):688–710. doi:10.1016/j.preteyeres.2007.08.001 [PubMed: 17889587]
32. Hammel N, Belghith A, Weinreb RN, Medeiros FA, Mendoza N, Zangwill LM. Comparing the Rates of Retinal Nerve Fiber Layer and Ganglion Cell–Inner Plexiform Layer Loss in Healthy Eyes and in Glaucoma Eyes. Am J Ophthalmol. 2017;178:38–50. doi:10.1016/j.ajo.2017.03.008 [PubMed: 28315655]
33. Leung CKS, Ye C, Weinreb RN, Yu M, Lai G, Lam DS. Impact of age-related change of retinal nerve fiber layer and macular thicknesses on evaluation of glaucoma progression. Ophthalmology. 2013;120(12):2485–2492. doi:10.1016/j.ophtha.2013.07.021 [PubMed: 23993360]
34. Nouri-Mahdavi K, Nowroozizadeh S, Nassiri N, et al. Macular ganglion cell/inner plexiform layer measurements by spectral domain optical coherence tomography for detection of early glaucoma and comparison to retinal nerve fiber layer measurements. Am J Ophthalmol. 2013;156(6). doi:10.1016/j.ajo.2013.08.001
35. Hood DC, Fortune B, Arthur SN, et al. Blood vessel contributions to retinal nerve fiber layer thickness profiles measured with optical coherence tomography. J Glaucoma. 2008;17(7):519–528. doi:10.1097/IJG.0b013e3181629a02 [PubMed: 18854727]

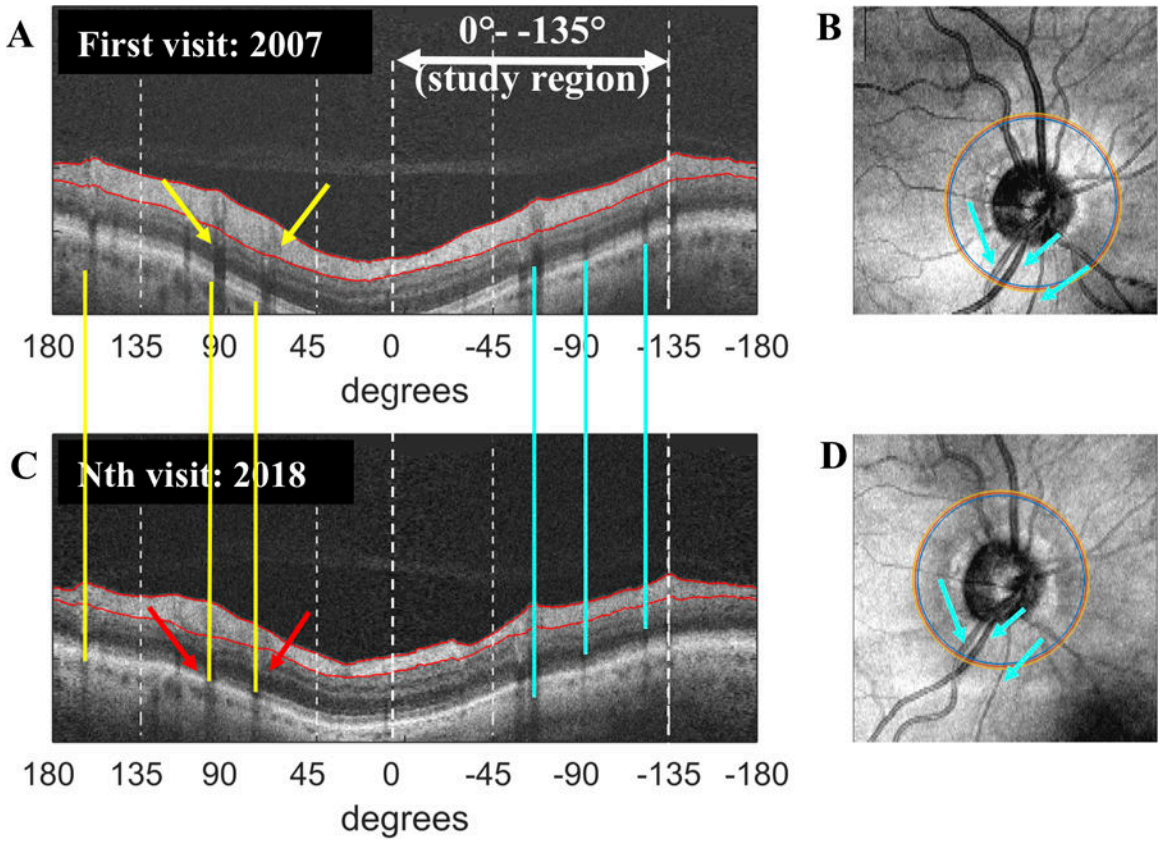

Figure 1:

Region of study and generating progression reports: An example of the custom-made progression report. (A and C) The derived circular b-scans are for the first and Nth visit. The blood vessels are aligned (blue vertical lines) in the study region (i.e., 0° [9 o'clock] to −135° [between 4 and 5 o'clock on right optic disc]). They are misaligned for the superior disc where the yellow vertical lines correctly fall on the shadows of the vessels in the lower panel (red arrows), but miss these in the upper panel (yellow arrows). (B and D) The enface images of the disc cube scans with the location of the derived circle scan from 2 different sessions were aligned using blood vessel landmarks (blue arrows in B and D, corresponding to blue vertical lines in 1A and C) to assure that the study region of each coincided. The eye shown corresponds to eye 1 in Fig. 3.

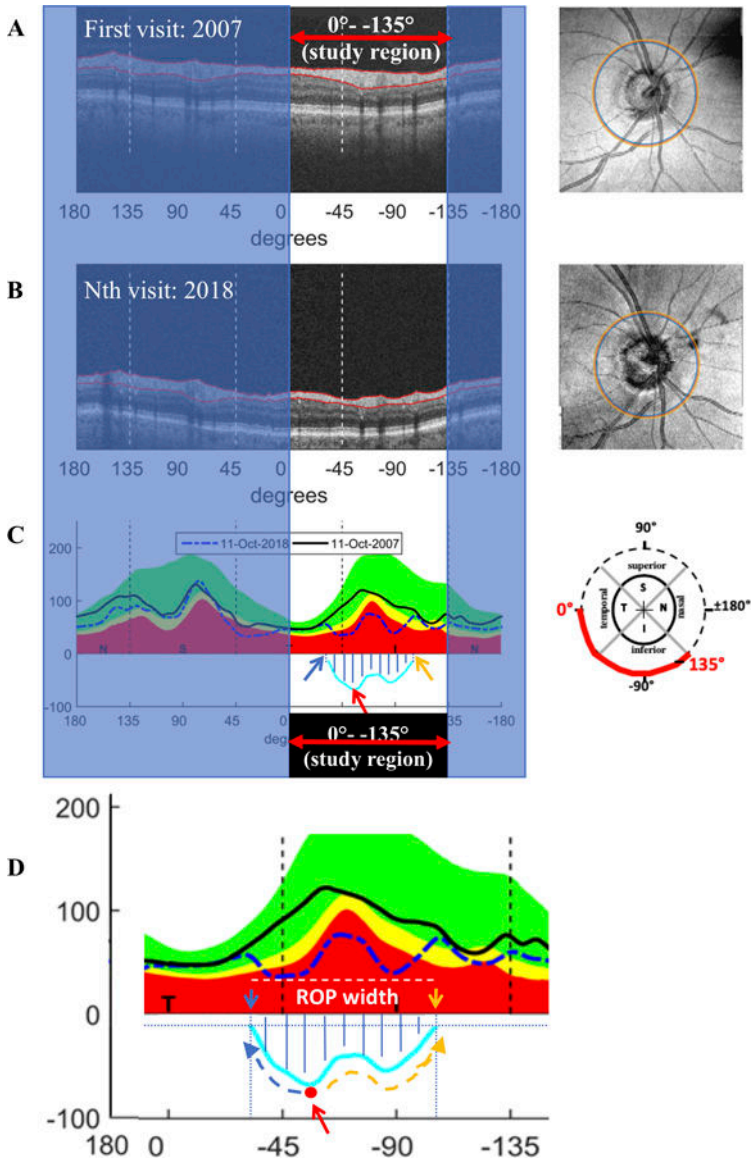

Figure 2:

Measuring changes in the region of progression (ROP). (A and B) The derived circular b-scans for two visits (left) and the enface image with the location of the derived circle scans (right panels of A and B). (C) A plot of the cRNFL thickness in the study region for the first (solid black curve) and Nth visit (dashed blue curve). The difference between them is shown as the light blue line at the bottom of the plot. (D) Enlarged image of study region in panel C. Red arrow indicates the location and amount of loss at the point of maximal loss. Starting from this point and moving along the difference curve to the left (blue dashed arrow) and to the right (orange dashed arrow), the leading (close to fixation, blue arrow) and trailing edges (orange arrow) were determined as the first location on the difference curve which fell below −5 μm. The ROP width was taken as the distance (in degrees) between the leading and trailing edges. Hatched region indicates the area of total loss in the ROP (μm^2). The eye shown corresponds to eye 11 in Fig. 3.

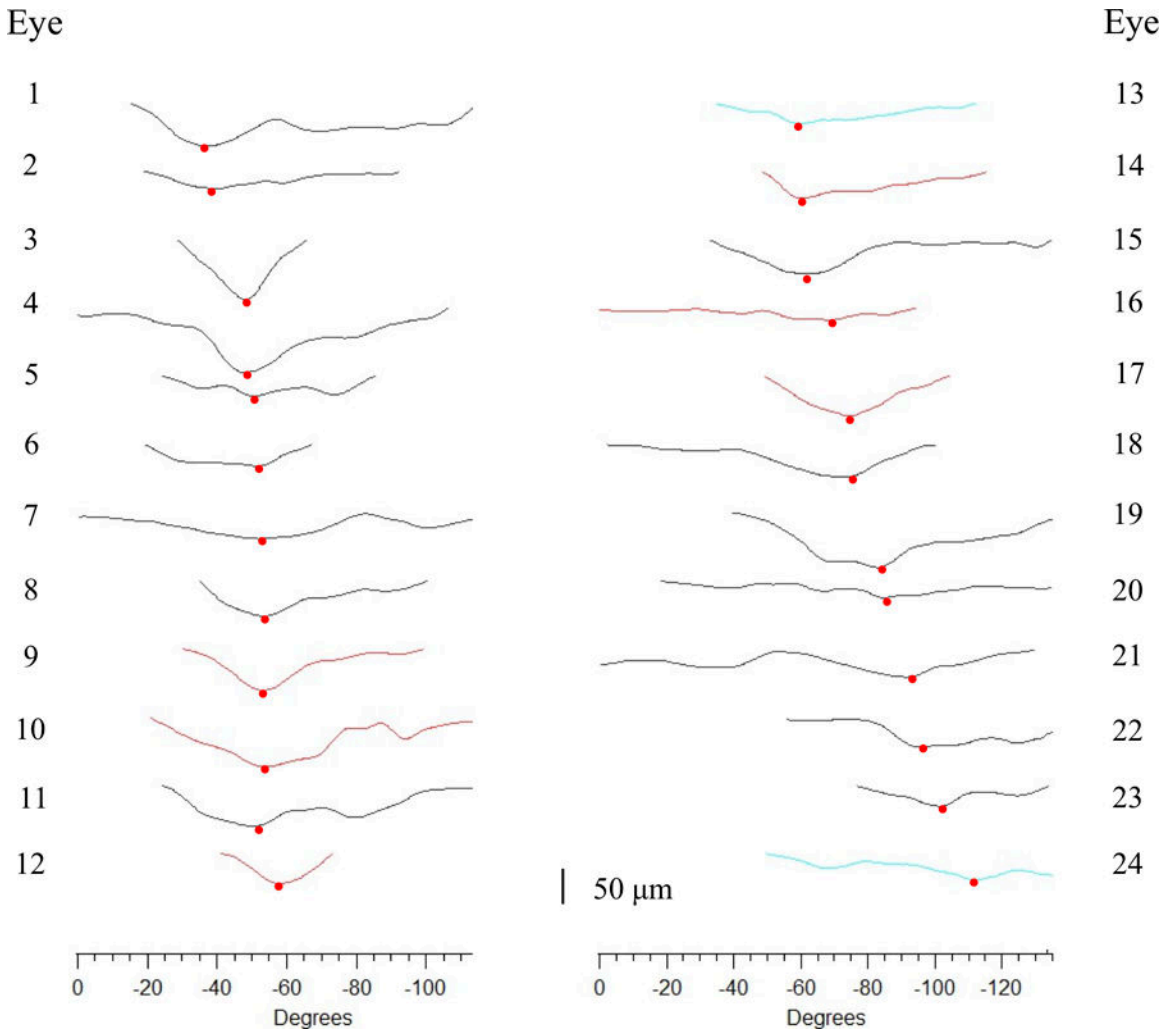

Figure 3:

ROP Width: The difference curve between the first and last scans for each of the 24 eyes plotted to scale (see bottom of figure for scale), ordered according to the location of the point of maximal loss. The ROP width is the width (in degrees) between the first and last points in each curve, which ranged from 32° to 131° (mean 82.7°±27.1°). Black indicates clinical diagnosis of primary open angle glaucoma; red indicates normal tension glaucoma, and blue secondary glaucoma due to pigmentary or exfoliation glaucoma.

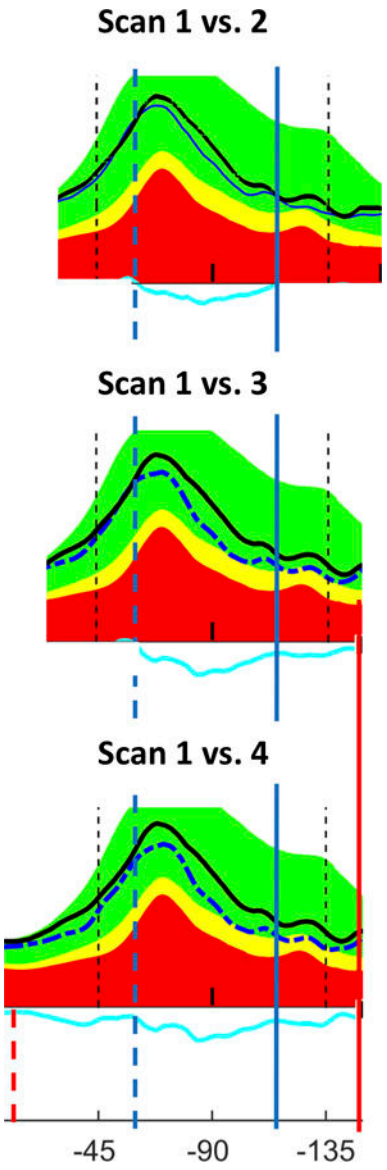

Figure 4:

Direction of progression relative to fixation: This figure shows eye 21 from Fig. 3 with progressive loss of cRNFL both towards fixation (leading edge) and in the opposite direction (trailing edge). The initial edges of the ROP are shown as the dark blue dashed (leading edge) and solid (trailing edge) vertical lines, and the final edges as the red vertical dashed and solid lines. Time between Scan 1 and Scan 2 is 8.4 years; Scan 1 vs. Scan 3 is 10.3 years; Scan 1 vs. Scan 4 is 11.4 years.

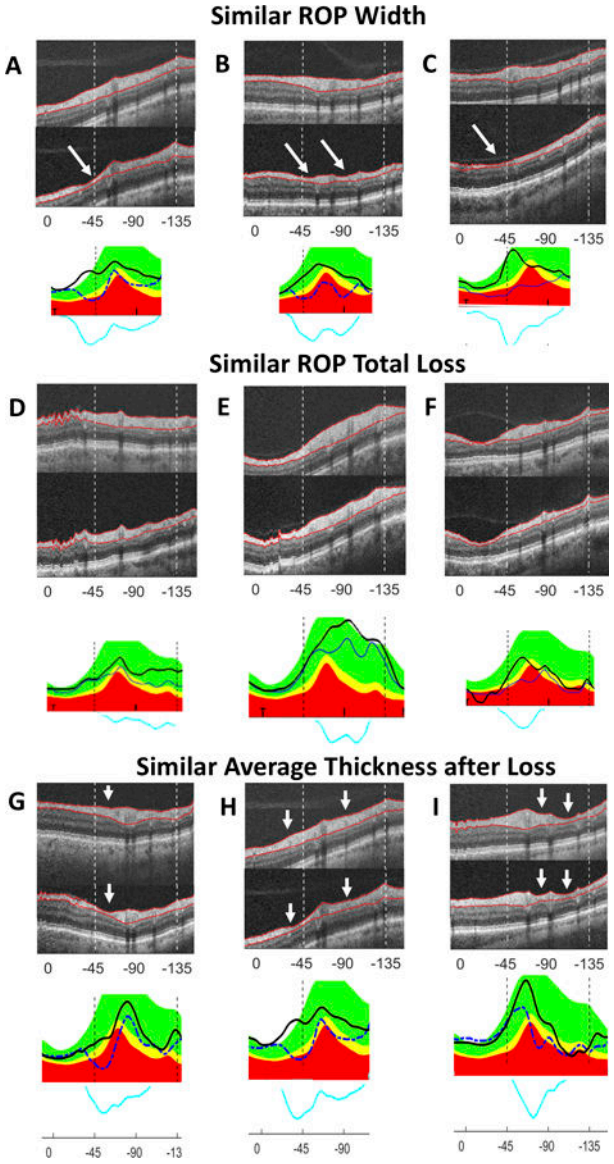

Figure 5:

(A–C) *Similar ROP width but different patterns:* Eyes with **similar ROP width** between first and last scans show different patterns of loss: **A** (eye 1 in Fig. 3)= **99.5°; B** (11)=**105.1°; C** (14)=**106.2°**. ***(D–F)*** *Similar ROP total loss but different patterns:* Eyes with **similar ROP total loss** (area under blue difference curve) show different patterns of loss: **D** (eye 24 in Fig. 3)**= 65,568.1 μm^2; E** (23)**= 67,708.7 μm^2; F** (15)**= 64,808.7 μm^2**. (D) showed wide loss which becomes deeper away from fixation, (E) showed a ROP of approximately equal thickness, and (F) showed a single deep area of local loss which is less wide than D or E. ***(G–I)*** *Similar average amount but different patterns of RNFL remaining in study region:* Eyes with similar **average cRNFL thicknesses remaining in the study region (0- −135°)** at the last scan dates demonstrate widely varying ROP width and depth: **G** (eye 8 in Fig. 3)= **70.6 μm; H** (1)= **69.4 μm; I** (17)= **67.8 μm**. (G) demonstrated loss towards 0° relative to the blood vessel, (H) showed loss on either side of blood vessels, and (I) showed loss on the side

of the blood vessels away from 0° (see white arrows). White arrows highlight variations in the width, number, and location of particularly deep areas of loss.